

Synthesis, crystal structures, magnetic properties and antimicrobial screening of octahedral nickel(II) complexes with substituted quinolin-8-olates and pyridine ligands

Tushar S. Basu Baul ^{a,*}, Khrawborlang Nongsiej ^a, Augustine Lamin Ka-Ot ^b, Santa Ram Joshi ^b, Bruno G.M. Rocha ^c, M. Fátima C. Guedes da Silva ^{c,**}

^a Centre for Advanced Studies in Chemistry, North-Eastern Hill University, NEHU Permanent Campus, Umshing, Shillong, 793 022, India

^b Department of Biotechnology & Bioinformatics, North-Eastern Hill University, NEHU Permanent Campus, Umshing, Shillong, 793 022, India

^c Centro de Química Estrutural, Complexo I, Instituto Superior Técnico, Universidade de Lisboa, Av. Rovisco Pais, 1049-001, Lisboa, Portugal



ARTICLE INFO

Article history:

Received 20 June 2019

Received in revised form

27 August 2019

Accepted 20 September 2019

Available online 24 September 2019

Keywords:

Substituted quinolin-8-olate

Nickel

Pyridine derivative

Magnetic moment

Structure elucidation

Antimicrobial activity

ABSTRACT

New nickel(II) compounds, viz. *trans*-[Ni(L^{XAO})₂(Py)₂]·C₆H₆ (**1**), *cis*-[Ni(L^{XAO})₂(3-MePy)₂] (**2**), *cis*-[Ni(L^{2-MeAO})₂(3-MePy)₂] (**3**), *trans*-[Ni(L^{4-MeAO})₂(Py)₂]·C₆H₆ (**4**), *trans*-[Ni(L^{4-OMeAO})₂(Py)₂]·C₆H₆ (**5**), *trans*-[Ni(L^{4-OEtAO})₂(Py)₂]·C₆H₆ (**6**), *trans*-[Ni(L^{4-BnAO})₂(Py)₂]·C₆H₆ (**7**) and *trans*-[Ni(L^{4-ClAO})₂(3-MePy)₂]·2(3-MePy) (**8**) (primary ligands: Py = pyridine or 3-MePy = 3-methylpyridine) have been synthesized and characterized by elemental analysis, IR, UV-vis spectroscopy. The magnetic susceptibilities of the compounds were also measured. Single-crystal X-ray diffraction analysis of the compounds revealed octahedral geometries with *trans* configurations for **1**, **4**–**8** and *cis* configurations for **2** and **3**. The occurrence of intramolecular Ni...H_{pyridine} interactions in **2** and in **3**, may account for additional stabilization of their assemblies at least in the solid state. The effective magnetic moment (μ_{eff}) in the range 3.02–3.40 BM agree with the expected values for octahedral Ni(II) cations with two unpaired electrons. Ni(II) compounds were also screened for their antimicrobial activity.

© 2019 Elsevier B.V. All rights reserved.

1. Introduction

Quinolin-8-ols (HL^Q) are good metal ion chelators [1–9] and their derivatives 2-(quinolin-8-yloxy)propionates, 5-aryl-8-hydroxyquinolines [10–12] and 8-aminoquinoline [13–16] were widely studied. Metal compounds of HL^Q were extensively used in photochemical processes [17–21], optical sensing [22–24] or as organic light-emitting diodes [25–29]. Other applications of HL^Q encompass thin film formation of nano-sized metal quinolin-8-olates [30] and nanobelt structures [31] involving 3d metals. The coordination behavior of 5-[(E)-2-(aryl)-1-diazenyl]-quinolin-8-ol (HL^{XAO}) towards M(II)/M(III) ions has been developed [32–39] with recent focus on their use as colorimetric sensors [40] as well as in the extraction of Cu(II) and Ni(II) at low concentrations [41].

Nanosized [Co(L^{XAO})₂] thin films with energy gaps of 4.01 eV [42], HL^{XAO} and its M(II) complexes as dyes in polyester fabrics [43], HL^{XAO}-Zn(II) complexes as zinc source for nano-structured materials [44], and promising non-linear optical behavior of some HL^{XAO} with 3d transition metal complexes [32d], are recent research developments.

Despite such progresses crystal structures of the HL^{XAO} complexes are scarce. The N- and O-atoms of HL^{XAO} as bidentate ligand can bind both medium and hard metal ions and give rise to different geometries. Two molecules of HL^{XAO} can give rise to square-planar (e.g., with Cu(II) ions) and tetrahedral complexes (e.g., with Cu(I) or Co(II) ions). Thus, for obtaining stable six coordinate octahedral metals complexes derived from HL^{XAO}, additional ancillary ligands such as pyridines are needed. Pyridine derivatives not only enhance solubility therefore ensuring the homogeneity of the reaction mixture, but also modulate the acidity of the metal center. On the basis of this hypothesis, the pro-ligands HL^{XAO} have been utilized for designing various types of discrete compounds, frequently involving Co(II) and Zn(II) cations with different

* Corresponding author.

** Corresponding author.

E-mail addresses: basubaulchem@gmail.com, basubaul@nehu.ac.in (T.S. Basu Baul), fatima.guedes@tecnico.ulisboa.pt (M.F.C. Guedes da Silva).

coordination numbers and geometries, giving rise to a large variety of structural motifs in the solid state with promising applications [44,45].

Nickel is an essential trace metal for animal species, plants and micro-organisms; it is also present in alloys and nickel-plated materials. However, this metal has shown adverse effects on human health through chronic exposure such as dermatitis, lung fibrosis, cardiovascular diseases, carcinogenic hazards, etc. [46,47]. The present work focuses on the synthesis, characterization and structure elucidation of a series of Ni(II) compounds based on HL^{XAO} pro-ligands in combination with pyridine derivatives as ancillary ligands. The chemical structure of the compounds, viz. *trans*- $[\text{Ni}(\text{L}^{\text{HAQ}})_2(\text{Py})_2] \cdot \text{C}_6\text{H}_6$ (**1**), *cis*- $[\text{Ni}(\text{L}^{\text{HAQ}})_2(3\text{-MePy})_2]$ (**2**), *cis*- $[\text{Ni}(\text{L}^{2\text{-MeAQ}})_2(3\text{-MePy})_2]$ (**3**), *trans*- $[\text{Ni}(\text{L}^{4\text{-MeAQ}})_2(\text{Py})_2] \cdot \text{C}_6\text{H}_6$ (**4**), *trans*- $[\text{Ni}(\text{L}^{4\text{-OMeAQ}})_2(\text{Py})_2] \cdot \text{C}_6\text{H}_6$ (**5**), *trans*- $[\text{Ni}(\text{L}^{4\text{-OEtAQ}})_2(\text{Py})_2] \cdot \text{C}_6\text{H}_6$ (**6**), *trans*- $[\text{Ni}(\text{L}^{4\text{-BrAQ}})_2(\text{Py})_2] \cdot \text{C}_6\text{H}_6$ (**7**) and *trans*- $[\text{Ni}(\text{L}^{4\text{-ClAQ}})_2(3\text{-MePy})_2] \cdot 2(3\text{-MePy})$ (**8**) (L^{XAO} = substituted 5-[*(E*)-2-(aryl)-1-diazenyl]quinolin-8-olate; Py = pyridine or 3-MePy = 3-methylpyridine) are outlined in **Scheme 1**. They were characterized by spectroscopic methods, including single crystal X-ray diffraction analysis. Magnetic susceptibility determinations in solution disclosed the octahedral geometry also in solution. The *in vitro* antimicrobial screening of compounds **1–8** is also reported.

2. Experimental

2.1. General considerations

$\text{Ni(OAc)}_2 \cdot 4\text{H}_2\text{O}$ (S.d. fine), 8-hydroxyquinoline (Loba Chemie), *o*-toluidine (SRL), *p*-ethoxyaniline, *p*-chloroaniline, *p*-bromoaniline (HiMedia), pyridine (Merck) and 3-methylpyridine (Spectrochem) were used without further purification. *p*-toluidine and *p*-anisidine

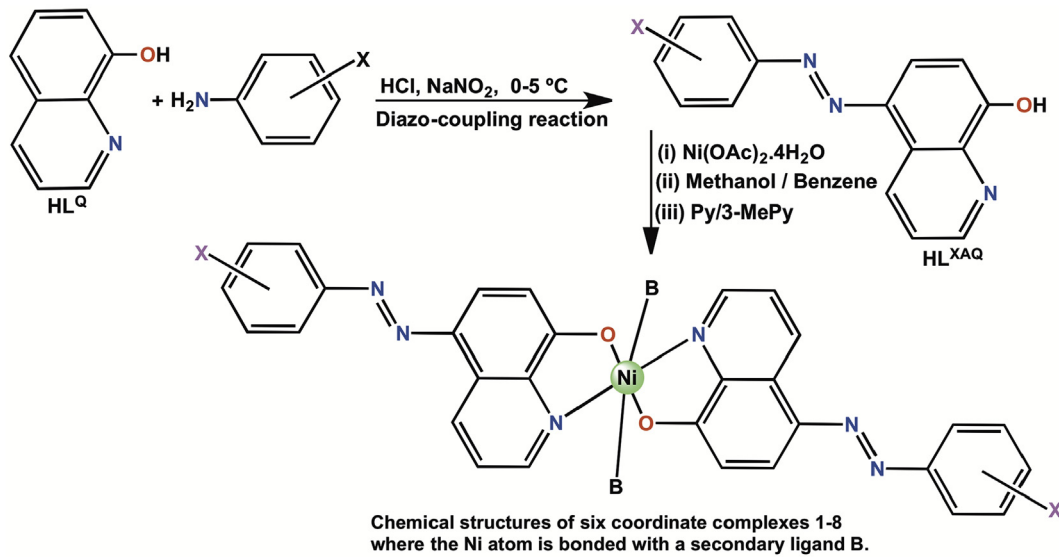
(CDH) were purified by crystallization and aniline (sd fine) was distilled prior to use. The solvents used in the reactions were of AR grade and dried using standard procedures.

Melting points were measured using a Büchi apparatus (M-560) and are uncorrected. Carbon, hydrogen and nitrogen analyses were performed with a PerkinElmer 2400 series II instrument. IR spectra in the range 4000–400 cm^{-1} were obtained on a PerkinElmer Spectrum BX series FT-IR spectrophotometer with samples investigated as KBr discs. Absorption measurements were carried out on a PerkinElmer Lambda 25 spectrophotometer at ambient temperature in freshly prepared DMSO solutions (**Table S1**; **Fig. S1**). The effective magnetic moments (μ_{eff}) were measured in solution by NMR on a Bruker Advance 300 spectrometer operating at 300.13 MHz (for **1–3**) or on a Bruker Advance 400 spectrometer operating at 400.13 MHz (for the remaining compounds), at room temperature in an open-air system. The Evans' method [48] was applied with measurements performed in standard 5 mm NMR tubes containing the paramagnetic sample dissolved in $\text{DMSO}-d_6$ and comprising a coaxial insert filled only with the same deuterated solvent. The ^1H chemical shifts were referred to the residual signals from this solvent as reference. The chemical shifts were measured in ppm. For the data treatment of NMR signals the MestReNova version 9.0.1 program was used.

For the *in vitro* antimicrobial assays, Mueller-Hinton agar (HiMedia) was used as nutrient liquid medium and standard antibiotic discs of chloramphenicol (C)³⁰ and fluconazole (FLC)²⁵ (HiMedia) were used as positive controls for bacteria and fungus, respectively.

2.2. Synthesis of pro-ligands and Ni(II) compounds

Pro-ligands 5-[*(E*)-2-(aryl)-1-diazenyl]quinolin-8-ol (HL^{XAO})



X	HL^{XAO}	B	Complex	Complex No.
H	HL^{HAQ}	Pyridine (Py)	$[\text{Ni}(\text{L}^{\text{HAQ}})_2(\text{Py})_2] \cdot \text{C}_6\text{H}_6$	1
2-Me	$\text{HL}^{2\text{-MeAQ}}$	3-Methylpyridine (3-MePy)	$[\text{Ni}(\text{L}^{\text{HAQ}})_2(3\text{-MePy})_2]$	2
4-Me	$\text{HL}^{4\text{-MeAQ}}$	3-Methylpyridine (3-MePy)	$[\text{Ni}(\text{L}^{2\text{-MeAQ}})_2(3\text{-MePy})_2]$	3
4-OMe	$\text{HL}^{4\text{-OMeAQ}}$	Pyridine (Py)	$[\text{Ni}(\text{L}^{4\text{-MeAQ}})_2(\text{Py})_2] \cdot \text{C}_6\text{H}_6$	4
4-OEt	$\text{HL}^{4\text{-OEtAQ}}$	Pyridine (Py)	$[\text{Ni}(\text{L}^{4\text{-OMeAQ}})_2(\text{Py})_2] \cdot \text{C}_6\text{H}_6$	5
4-Br	$\text{HL}^{4\text{-BrAQ}}$	Pyridine (Py)	$[\text{Ni}(\text{L}^{4\text{-OEtAQ}})_2(\text{Py})_2] \cdot \text{C}_6\text{H}_6$	6
4-Cl	$\text{HL}^{4\text{-ClAQ}}$	3-Methylpyridine (3-MePy)	$[\text{Ni}(\text{L}^{4\text{-BrAQ}})_2(\text{Py})_2] \cdot \text{C}_6\text{H}_6$	7
			$[\text{Ni}(\text{L}^{4\text{-ClAQ}})_2(3\text{-MePy})_2] \cdot 2(3\text{-MePy})$	8

Scheme 1. Synthesis of pro-ligand HL^{XAO} and chemical structures of the nickel(II) compounds **1–8**.

viz., 5-[*(E*)-2-(phenyl)-1-diazenyl]quinolin-8-ol (HL^{HAQ}), 5-[*(E*)-2-(2-methylphenyl)-1-diazenyl]quinolin-8-ol ($\text{HL}^{2-\text{MeAQ}}$), 5-[*(E*)-2-(4-methylphenyl)-1-diazenyl]quinolin-8-ol ($\text{HL}^{4-\text{MeAQ}}$), 5-[*(E*)-2-(4-ethoxyphenyl)-1-diazenyl]quinolin-8-ol ($\text{HL}^{4-\text{OEtAQ}}$), 5-[*(E*)-2-(4-bromophenyl)-1-diazenyl]quinolin-8-ol ($\text{HL}^{4-\text{BrAQ}}$) [35e] and 5-[*(E*)-2-(4-methoxyphenyl)-1-diazenyl]quinolin-8-ol ($\text{HL}^{4-\text{OMeAQ}}$) and 5-[*(E*)-2-(4-chlorophenyl)-1-diazenyl]quinolin-8-ol ($\text{HL}^{4-\text{ClAQ}}$) [35d] were prepared starting from 8-hydroxyquinoline and the corresponding aniline using conventional diazonium salt chemistry, in accordance with literature procedures. In view of the similar preparation methods employed for **1–8**, only the preparation for $[\text{Ni}(\text{L}^{\text{HAQ}})_2(\text{Py})_2] \cdot \text{C}_6\text{H}_6$ (**1**) is described in detail, as a representative example.

2.2.1. Synthesis of trans-bis{5-[*(E*)-2-(phenyl)-1-diazenyl]quinolin-8-olato- $k^2\text{N},\text{O}$ }-bis(pyridine-*kN*) nickel(II) benzene solvate (**1**)

$\text{Ni}(\text{OAc})_2 \cdot 4\text{H}_2\text{O}$ (0.249 g, 1.00 mmol) in methanol (10 mL) was added drop-wise to a stirred solution of HL^{HAQ} (0.5 g, 2.00 mmol) in benzene (50 mL) at room temperature, which resulted in the immediate formation of a reddish-orange precipitate. The reaction mixture was heated to reflux for 3 h and then filtered while hot. The residue was washed with hot methanol (3×5 mL) to remove undesired materials and dried *in vacuo*. The dried solid was dissolved in hot benzene (10 mL) containing pyridine (0.8 mL, 10.11 mmol) and filtered while hot. The filtrate was diluted with toluene (1 mL) and upon slow evaporation reddish-brown crystals of **1** were obtained. Yield: 0.48 g (60%; relative to nickel acetate). M.p. > 300 °C. Anal. Found: C, 70.10; H, 4.88; N, 14.08%. Calc. for $\text{C}_{46}\text{H}_{36}\text{N}_8\text{NiO}_2$ (MW = 791.52 gmol⁻¹): C, 69.80; H, 4.58; N, 14.16%. IR (cm⁻¹): 1597 m, 1573 m, 1552 m, 1500s, 1465s, 1393s, 1331s, 1249s, 1187 m, 1131 m, 1100 m, 764w, 702 m, 684w, 464w. Electronic absorption data (DMSO) λ_{max} , nm; (ϵ [M⁻¹ cm⁻¹]): 440 sh, 499 (11602).

2.2.2. Synthesis of cis-bis{5-[*(E*)-2-(phenyl)-1-diazenyl]quinolin-8-olato- $k^2\text{N},\text{O}$ }-bis(3-methyl pyridine-*kN*) nickel(II) (**2**)

$\text{Ni}(\text{OAc})_2 \cdot 4\text{H}_2\text{O}$ (0.249 g, 1.00 mmol) and HL^{HAQ} (0.5g, 2.00 mmol) were used in the reaction. The dried solid was dissolved by heating the benzene solution (10 mL) containing 3-methylpyridine (1 mL, 10.73 mmol) and filtered while hot. The filtrate upon slow evaporation yielded reddish-brown crystals. Yield: 0.48 g (64%; relative to nickel acetate). M.p. > 300 °C. Anal. Found: C, 68.32; H, 4.68; N, 14.88. Calc. for $\text{C}_{42}\text{H}_{34}\text{N}_8\text{NiO}_2$ (MW 741.47 gmol⁻¹): C, 68.03; H, 4.62; N, 15.11%. IR (cm⁻¹): 1596 m, 1570 m, 1551 m, 1498s, 1469s, 1400s, 1330s, 1247s, 1188 m, 1167 m, 1132 m, 831w, 787 m, 764w, 690w, 507w. Electronic absorption data (DMSO) λ_{max} , nm; (ϵ [M⁻¹ cm⁻¹]): 439 sh, 499 (16802).

2.2.3. Synthesis of cis-bis{5-[*(E*)-2-(2-methylphenyl)-1-diazenyl]quinolin-8-olato- $k^2\text{N},\text{O}$ }-bis(3-methylpyridine-*kN*) nickel(II) (**3**)

$\text{Ni}(\text{OAc})_2 \cdot 4\text{H}_2\text{O}$ (0.236 g, 0.95 mmol) and $\text{HL}^{2-\text{MeAQ}}$ (0.5 g, 1.90 mmol) were used in the reaction. The dried solid was dissolved by heating the benzene solution (10 mL) containing 3-methylpyridine (1 mL, 10.74 mmol) and filtered while hot. The filtrate upon slow evaporation yielded reddish-brown crystals. Yield: 0.46 g (63%; relative to nickel acetate). M.p. > 300 °C. Anal. Found: C, 68.72; H, 4.76; N, 14.50. Calc. for $\text{C}_{44}\text{H}_{38}\text{N}_8\text{NiO}_2$ (MW 769.52 gmol⁻¹): C, 68.68; H, 4.98; N, 14.56%. IR (cm⁻¹): 1595 m, 1571 m, 1554 m, 1498s, 1470s, 1402s, 1329s, 1245s, 1181 m, 1168 m, 1109w, 791 m, 762 m, 704w, 459w. Electronic absorption data (DMSO) λ_{max} , nm; (ϵ [M⁻¹ cm⁻¹]): 439 sh, 501 (9388).

2.2.4. Synthesis of trans-bis{5-[*(E*)-2-(4-methylphenyl)-1-diazenyl]quinolin-8-olato- $k^2\text{N},\text{O}$ }-bis(pyridine-*kN*) nickel(II) benzene solvate (**4**)

$\text{Ni}(\text{OAc})_2 \cdot 4\text{H}_2\text{O}$ (0.236 g, 0.95 mmol) and $\text{HL}^{4-\text{MeAQ}}$ (0.5 g,

1.89 mmol) were used in the reaction. The dried solid was dissolved by heating the chloroform solution (10 mL) containing pyridine (0.8 mL, 10.11 mmol) and filtered to remove any suspended particles. The filtrate was diluted with benzene (1 mL), which upon slow evaporation afforded reddish-brown crystals. Yield: 0.48 g (61%; relative to nickel acetate). M.p. > 300 °C. Anal. Found: C, 70.30; H, 5.28; N, 14.02. Calc. for $\text{C}_{42}\text{H}_{34}\text{N}_8\text{NiO}_2$ (MW 819.58 gmol⁻¹): C, 70.34; H, 4.92; N, 13.67%. IR (cm⁻¹): 1597 m, 1574 m, 1551 m, 1498s, 1465s, 1392 m, 1329s, 1246s, 1188w, 1169w, 1100w, 793w, 760w, 704w, 463w. Electronic absorption data (DMSO) λ_{max} , nm; (ϵ [M⁻¹ cm⁻¹]): 440 sh, 499 (14616).

2.2.5. Synthesis of trans-bis{5-[*(E*)-2-(4-methoxyphenyl)-1-diazenyl]quinolin-8-olato- $k^2\text{N},\text{O}$ }-bis(pyridine-*kN*) nickel(II) benzene solvate (**5**)

$\text{Ni}(\text{OAc})_2 \cdot 4\text{H}_2\text{O}$ (0.22 g, 0.89 mmol) and $\text{HL}^{4-\text{OMeAQ}}$ (0.5 g, 1.79 mmol) were used in the reaction. The dried solid was dissolved by heating the benzene solution (15 mL) containing pyridine (0.8 mL, 10.11 mmol) and filtered while hot. The filtrate upon slow evaporation yielded reddish-brown crystals. Yield: 0.47 g (61%; relative to nickel acetate). M.p. > 300 °C. Anal. Found: C, 67.37; H, 5.12; N, 13.23. Calc. for $\text{C}_{42}\text{H}_{34}\text{N}_8\text{NiO}_4$ (MW 851.58 gmol⁻¹): C, 67.70; H, 4.73; N, 13.16%. IR (cm⁻¹): 1595 m, 1573 m, 1552 m, 1496s, 1463s, 1391 m, 1328s, 1244s, 1190 m, 1170 m, 1099w, 832w, 759w, 703w, 472w. Electronic absorption data (DMSO) λ_{max} , nm; (ϵ [M⁻¹ cm⁻¹]): 437 sh, 503 (13531).

2.2.6. Synthesis of trans-bis{5-[*(E*)-2-(4-ethoxyphenyl)-1-diazenyl]quinolin-8-olato- $k^2\text{N},\text{O}$ }-bis(pyridine-*kN*) nickel(II) benzene solvate (**6**)

$\text{Ni}(\text{OAc})_2 \cdot 4\text{H}_2\text{O}$ (0.212 g, 0.85 mmol) and $\text{HL}^{4-\text{OEtAQ}}$ (0.50 g, 1.70 mmol) were used in the reaction. The dried solid was dissolved by heating the benzene solution (10 mL) containing pyridine (0.8 mL, 10.11 mmol) and filtered while hot. The filtrate upon slow evaporation yielded reddish-brown crystals. Yield: 0.45 g (60%; relative to nickel acetate). M.p. > 300 °C. Anal. Found: C, 68.52; H, 5.01; N, 12.58. Calc. for $\text{C}_{44}\text{H}_{38}\text{N}_8\text{NiO}_4$ (MW 879.63 gmol⁻¹): C, 68.27; H, 5.04; N, 12.74%. IR (cm⁻¹): 1638w, 1596 m, 1571s, 1495s, 1468s, 1402 m, 1322s, 1235s, 1191 m, 1098 m, 1041 m, 920w, 838 m, 767w, 697w, 476w. Electronic absorption data (DMSO) λ_{max} , nm; (ϵ [M⁻¹ cm⁻¹]): 439 sh, 503 (16173).

2.2.7. Synthesis of trans-bis{5-[*(E*)-2-(4-bromophenyl)-1-diazenyl]quinolin-8-olato- $k^2\text{N},\text{O}$ }-bis(pyridine-*kN*) nickel(II) benzene solvate (**7**)

$\text{Ni}(\text{OAc})_2 \cdot 4\text{H}_2\text{O}$ (0.189 g, 0.76 mmol) and $\text{HL}^{4-\text{BrAQ}}$ (0.5 g, 1.523 mmol) were used in the reaction. The dried solid was dissolved by heating the chloroform solution (20 mL) containing pyridine (0.8 mL, 10.113 mmol) and filtered to remove any suspended particles. The filtrate was diluted with benzene (1 mL) which upon slow evaporation yielded reddish-brown crystals. Yield: 0.46 g (63%; relative to nickel acetate). M.p. > 300 °C. Anal. Found: C, 57.80; H, 3.66; N, 12.28. Calc. for $\text{C}_{40}\text{H}_{28}\text{Br}_2\text{N}_8\text{NiO}_2$ (MW 949.32 gmol⁻¹): C, 58.20; H, 3.61; N, 11.80%. IR (cm⁻¹): 1597 m, 1573 m, 1549 m, 1500 m, 1464s, 1407 m, 1380 m, 1327s, 1297 m, 1248s, 1187 m, 1167 m, 1131 m, 1100w, 828w, 791w, 702w, 465w. Electronic absorption data (DMSO) λ_{max} , nm; (ϵ [M⁻¹ cm⁻¹]): 440 sh, 510 (11396).

2.2.8. Synthesis of trans-bis{5-[*(E*)-2-(4-chlorophenyl)-1-diazenyl]quinolin-8-olato- $k^2\text{N},\text{O}$ }-bis(3-methylpyridine-*kN*) nickel(II) 3-methylpyridine disolvates (**8**)

$\text{Ni}(\text{OAc})_2 \cdot 4\text{H}_2\text{O}$ (0.219 g, 0.88 mmol) and $\text{HL}^{4-\text{ClAQ}}$ (0.5 g, 1.76 mmol) were used in the reaction. The dried solid was dissolved by heating the benzene solution (10 mL) containing 3-

Table 1Crystal data, data collection parameters and convergence results for compounds **1–8**.

	1	2	3	4	5	6	7	8
Empirical formula	C ₄₆ H ₃₆ N ₈ NiO ₂	C ₄₂ H ₃₄ N ₈ NiO ₂	C ₄₄ H ₃₈ N ₈ NiO ₂	C ₄₈ H ₄₀ N ₈ NiO ₂	C ₄₈ H ₄₀ N ₈ NiO ₄	C ₅₀ H ₄₄ N ₈ NiO ₄	C ₄₆ H ₃₄ Br ₂ N ₈ NiO ₂	C ₅₄ H ₄₆ Cl ₂ N ₁₀ NiO ₂
Formula weight	791.54	741.48	769.53	819.59	851.59	879.64	949.34	996.62
Crystal system	triclinic	monoclinic	triclinic	triclinic	triclinic	triclinic	triclinic	triclinic
Space group	P –1	I 2/a	P –1	P –1				
<i>a</i> (Å)	8.5734(4)	17.2498(19)	7.9744(8)	8.3564(7)	8.4401(6)	9.2322(10)	8.3320(4)	9.5962(8)
<i>b</i> (Å)	10.4854(5)	14.9060(13)	16.2187(10)	10.9537(5)	11.2127(8)	10.5635(11)	11.0173(6)	11.2381(9)
<i>c</i> (Å)	10.8215(5)	16.5869(15)	17.6853(8)	11.3606(6)	11.3145(8)	12.1003(12)	11.3430(6)	12.4662(10)
α (°)	93.587(4)	90	98.049(5)	98.660(4)	100.102(6)	74.593(9)	99.082(4)	105.768(7)
β (°)	92.700(4)	101.594(11)	99.704(6)	91.250(5)	93.302(7)	72.044(8)	91.473(3)	94.026(6)
γ (°)	92.693(4)	90	97.282(7)	95.885(5)	93.514(6)	84.193(7)	95.433(4)	106.939(7)
<i>V</i> (Å ³)	968.60(8)	4177.9(7)	2205.7(3)	1021.87(11)	1049.63(13)	1082.0(2)	1022.70(9)	1221.27(18)
<i>Z</i>	1	4	2	1	1	1	1	1
<i>D</i> _{calc} (g/cm ³)	1.357	1.179	1.159	1.332	1.347	1.350	1.541	1.355
F000	412	1544	804	428	444	460	480	518
μ (mm ⁻¹)	0.552	0.507	0.483	0.525	0.518	0.505	2.478	0.560
Reflections measured	7476	8505	17080	7894	4562	7786	7961	9048
Obs/Unique reflections	4359/3412	4852/3053	9738, 5493	4599, 3937	3696/2981	4900/3242	4631, 3217	5478, 3405
Number of parameters	287	240	500	284	293	302	268	315
<i>R</i> _{int}	0.0244	0.0454	0.1121	0.0308	0.0173	0.0446	0.0308	0.0414
<i>R</i> (<i>F</i>) (<i>I</i> ≥ 2σ)	0.0465	0.0636	0.0836	0.0470	0.0635	0.0704	0.0533	0.0673
wR (<i>F</i> ²) (all data)	0.1196	0.1871	0.2234	0.1132	0.1435	0.1587	0.1158	0.1209
GOF (<i>F</i> ²)	0.842	0.786	0.926	1.057	1.331	1.038	1.166	1.020
max., min. Δ <i>p</i> (e/Å ³)	0.335, –0.175	0.861, –0.323	1.151, –0.824	0.372, –0.421	0.989, –0.455	0.755, –0.509	0.879, –0.646	0.342, –0.251

methylpyridine (1 mL, 10.74 mmol) and filtered. The filtrate upon slow evaporation yielded reddish-brown crystals. Yield: 0.46 g (52%; relative to nickel acetate). M.p. > 300 °C. Anal. Found: C, 64.82; H, 4.60; N, 14.22. Calc. for C₄₂H₃₂Cl₂N₈NiO₂ (MW 996.61 g/mol⁻¹): C, 65.08; H, 4.65; N, 14.05%. IR (cm⁻¹): 1596s, 1570s, 1552 m, 1500s, 1469s, 1410 m, 1384 m, 1327s, 1298 m, 1247s, 1188 m, 1170 m, 1132 m, 1084 m, 835 m, 792 m, 706 m, 518w, 467 m. Electronic absorption data (DMSO) λ_{max} , nm; (ϵ [M⁻¹ cm⁻¹]): 440 sh, 508 (10663).

2.3. X-ray crystallography

The measurements were performed on an Agilent Technologies four-circle Gemini diffractometer [49] using Mo K α radiation ($\lambda = 0.71073$ Å) from a fine-focus X-ray source. Full spheres of data were collected using omega scans of 0.5° per frame and data reduction was performed with CrysAlisPro [50]. Intensities were corrected for Lorentz and polarization effects and empirical absorption corrections using spherical harmonics were applied [50]. The structures were solved by direct methods using SIR97 package [51] and refined with SHELXL-2018/1 [52]. Calculations were performed using the WinGX System-Version 2014-1 [53]. Coordinates of hydrogen atoms, all bonded to carbon atoms, were included in the refinement using the riding-model approximation with the Uiso(H) defined as 1.2 Ueq of the parent aromatic and methylene

atoms, and 1.5U_{eq} of the parent carbon atoms for methyl. Least square refinements with anisotropic thermal motion parameters for all the non-hydrogen atoms were employed. In **5**, the low quality of the crystals gave rise to weak diffraction, particularly at high angles, leading to a relatively low data completeness. However, the observed data proves the structure and hence it is included for comparison purposes. Compounds **4** and **7** are isomorphs.

In compound **2** Platon/Squeeze routine [54] was used to account for disordered molecules in voids; two void contents of 424 Å³ and 86 electrons each (total of 856 Å³ with 171 electrons) were found, that fit well for two molecules of benzene in each. The model did not fit so well for 3-methylpyridine (1.7 molecules per void) but a mixture of both solvents is not to be disregarded. Platon/Squeeze [54] was also applied to compound **3** to deal with two void contents of 200 Å³ with 56 electrons in each (total of 400 Å³ with 113 electrons), that fit well for one molecule of 3-methylpyridine in each; the possibility of having a mixture of both benzene and 3-methylpyridine was also favorable. Upon using this procedure, the final R1 values improved from 0.0905 to 0.0636 (in **2**) and from 0.1111 to 0.0836 (in **3**).

In compounds **4–6** only half of the benzene molecule was located. In view of the unreasonable arrangement of the benzene molecule caused by the proximity to an inversion centre, the symmetry related carbon ring atoms were generated, the site

Table 2Selected bond distances (Å) and angles (°) for **1–8**.

	1	2	3	4	5	6	7	8
Geometric parameters for octahedral structure ^a	1.008 25.45	1.009 30.39	1.016 50.26	1.008 23.44	1.008 24.07	1.007 23.90	1.008 24.09	1.008 24.78 ⁻²
NN	1.258(3)	1.247(4)	1.265(7), 1.280(7)	1.257(3)	1.257(5)	1.259(4)	1.251(4)	1.265(3)
Ni–N _{quinoline}	2.060(2)	2.087(3)	2.190(4), 2.225(4)	2.0517(17)	2.056(3)	2.063(3)	2.049(3)	2.059(3)
Ni–N _{pyridine}	2.148(2)	2.112(3)	2.153(4), 2.168(4)	2.1536(18)	2.151(3)	2.134(3)	2.145(3)	2.152(2)
Ni–O	2.0500(15)	2.030(2)	2.066(4), 2.069(4)	2.0473(14)	2.045(2)	2.039(2)	2.050(2)	2.0353(19)
∠ O–Ni–N _{quinoline}	81.65(7)	80.55(10)	78.02(15), 78.39(15)	82.02(6)	81.92(10)	82.03(10)	81.87(10)	81.78(9)
P angle ^b	5.25	27.94	10.61 31.81	5.42	5.77	25.12	6.02	23.85
Q angle ^c	89.98	39.28	15.53 27.22	85.57	88.23	82.34	86.39	86.13
Shortest Ni...Ni	8.573	8.907	7.974	8.356	8.440	9.232	8.332	9.596

^a Values refer to quadratic elongation and angle variance (in °²), in this order, according to K. Robinson et al. [56].^b Angle between the least-square planes of quinoline and phenyl moieties in the azo-ligand.^c Angle between the least-square planes of quinoline and pyridine ligands.

Table 3
Non-classical H-bond interactions in **2–8**.

	H...A (Å)	D...A (Å)	D–H...A (°)	Symmetry operation
1				
C19–H19...O1	2.70	3.617(3)	171.3	$1 + x,y,z$
2				
C16–H16...Ni1	2.99	3.00	80.13	intra
C7–H7...O1	2.59	3.407(6)	147	$-x,-1/2 + y,1/2-z$
C16–H16...O1	2.46	2.963(5)	114	intra
3				
C39–H39...Ni1	2.99	3.02	78.99	intra
C14–H14...N2	2.50	2.810(8)	100	intra
C37–H37...O1	2.45	3.009(6)	118	intra
C43–H43...O2	2.54	3.090(6)	118	intra
4				
C18–H18...O1	2.59	3.510(3)	173	$-x,1-y,-z$
5				
C17–H17...Ni1	3.02	3.04	80.20	intra
C17–H17...O1	2.58	3.068(5)	113	intra
6				
C2–H2...O2	2.65	3.571(5)	173	$x,y,1 + z$
C18–H18...O1	2.51	3.045(5)	117	intra
C22–H22...O1	2.50	3.030(5)	116	intra
7				
C16–H16...O1	2.58	3.055(5)	112	intra
C19–H19...O1	2.59	3.508(5)	171	$-x,1-y,-z$
C17–H17...N3	2.72	3.639(5)	170	$x,y,-1+z$
8				
C16–H16...O1	2.56	3.061(4)	114	intra

occupancies of all the carbon atoms of benzene changed to 0.5 affording, because of this strategy, the whole molecule with occupancy of 0.5 as defined by the multiplicity of the special position. The atoms were then flanked by PART -1 and PART 0 and the

structure finalized normally, through the application of geometric restraints (e.g., AFIX 66). Crystallographic data, selected bond lengths and angles and hydrogen-bond interactions are given in Tables 1–3, respectively. The ellipsoid plots of all compounds with partial numbering schemes are shown in Figs. 1 and 2. Non-covalent interactions and packing diagrams are exemplified in Figs. S2–S6.

2.4. In vitro antimicrobial assay

The antimicrobial activity of pro-ligands HL^{XAO} and the corresponding Ni(II) compounds **1–8** were tested against three indicator bacterial strains, i.e., *Bacillus subtilis* MTCC 441, *Staphylococcus aureus* MTCC 96 and *Klebsiella pneumoniae* MTCC 109, and one fungal strain, *Candida albicans* MTCC 183, employing the agar well diffusion method [55].

The stock solutions for pro-ligands HL^{XAO} and compounds **1–8** were freshly prepared in DMSO prior to use. The stock concentrations of the tested samples were ~10,000 µg/mL. Mueller-Hilton agar plates were swabbed with bacterial cell suspensions of the indicator bacterial strains adjusted to 1.5×10^8 colony forming units (CFU)/mL. Then, the agar surface was bored by using a sterilized cork borer to generate wells of 5 mm diameter, which were filled with a 100 µL aliquot of the corresponding test compound solution. A disc with the broad-spectrum antibiotic chloramphenicol (30 mcg) was used as positive control and a DMSO solution as negative control. Plates were incubated at 37 °C for 24 h and the inhibition zones (mm) formed around the wells were measured using a Vernier caliper. For each organism, the experiments were conducted in triplicate and the antibacterial activity was evaluated

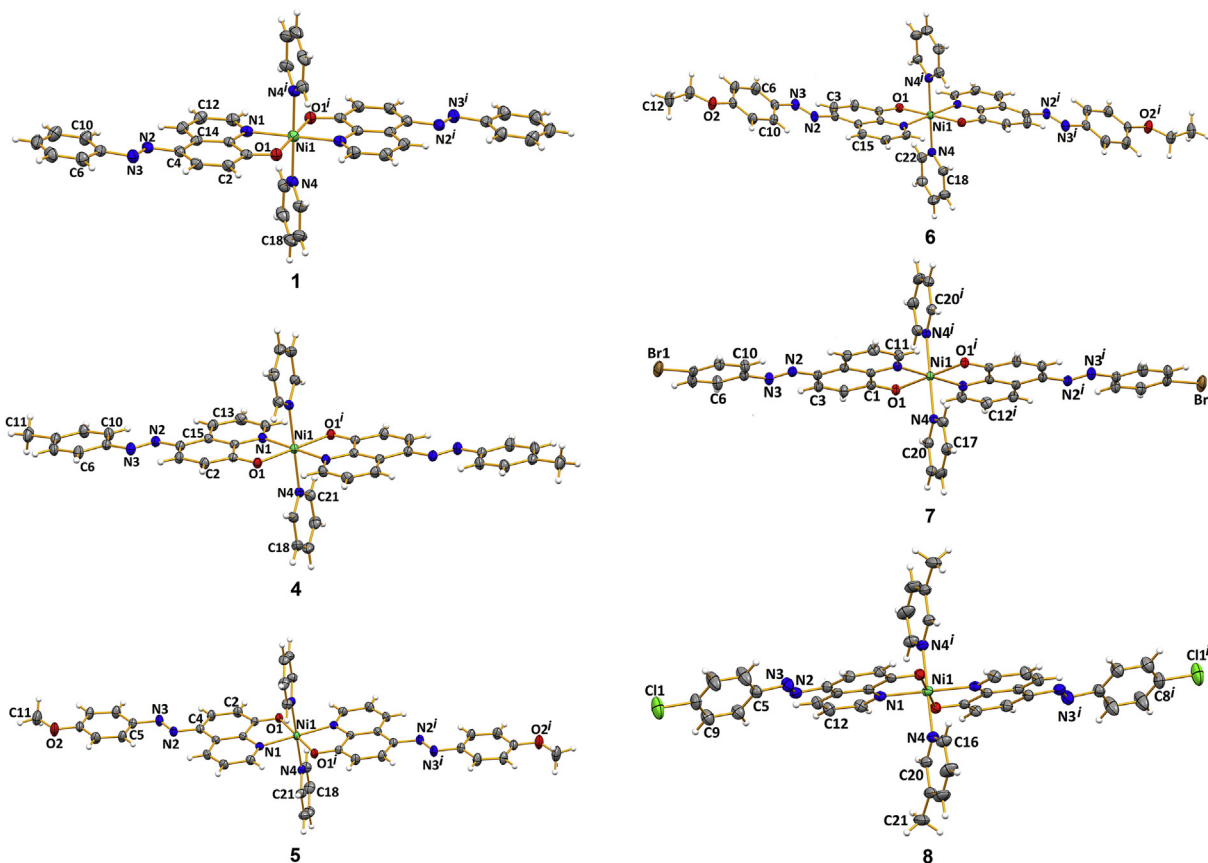


Fig. 1. Ellipsoid plot (drawn at 30% probability level) of the *trans*-nickel compounds **1**, **4–8** with partial atom labeling schemes. The solvent molecules are omitted for clarity. Symmetry operation to generate equivalent atoms: $2-x,2-y,-z$ (**1**); $1-x,1-y,-z$ (**4**, **7**); $2-x,-y,2-z$ (**5**); $-x,1-y,2-z$ (**6**); $2-x,1-y,2-z$ (**8**).

by measuring the growth inhibition zone diameter.

3. Results and discussion

3.1. Synthesis and spectroscopic characterization

Nickel(II) compounds were prepared by reacting a solution of $\text{Ni}(\text{OAc})_2 \cdot 4\text{H}_2\text{O}$ in methanol with HL^{XAO} dissolved in benzene in 1:2 mole ratios. In all cases a precipitate immediately formed. After suitable work up procedures, characterization of the isolated precipitates suggested compounds of general formula $[\text{Ni}(\text{L}^{\text{XAO}})_2]$. They were insoluble in methanol, ethanol, chloroform, methylene dichloride, benzene, toluene and acetone even after prolonged heating, but soluble in DMSO, pyridine and pyridine derivatives. Crystallization experiments of $[\text{Ni}(\text{L}^{\text{XAO}})_2]$ using sole DMSO, pyridine or pyridine derivatives afforded pasty materials which could not be worked up. However, when such crystallization experiments were attempted with a large excess of pyridine or pyridine derivatives in combination with other common solvents, reddish-brown crystalline materials were invariably obtained. Compounds **1**, **4–7** crystallized as benzene solvates, **8** as 3-methylpyridine disolvates, **2** and **3** were unsolvated (see Scheme 1). It should be mentioned that crystallization experiments were carried out under identical conditions with pyridine and 2-/3-/4-methylpyridine, but only a specific N-base provided a crystalline product, as detailed in Scheme 1. In all the compounds, the adduct formation of $\{\text{Ni}(\text{L}^{\text{XAO}})_2\}$ generated the six-coordinate complexes **1–8** with the participation of 2 mol equivalents of pyridine or 3-methylpyridine, as ascertained by elemental analyses and by X-ray diffraction. The characteristic IR and electronic absorption data are given in the Experimental section.

3.2. Description of the X-ray crystal structures

Crystals of the nickel(II) compounds, **1** (pyridine/benzene/toluene), **2**, **3** and **8** (3-methylpyridine/benzene), **4** and **7** (pyridine/benzene/chloroform), **5** and **6** (pyridine/benzene), suitable for single-crystal X-ray structure determination were obtained by slow evaporation of solutions of the respective compounds.

The asymmetric unit of the compounds include half of the complex molecule (**3** is the exception) and half a benzene (in **1**, **4–7**) or a full 3-methylpyridine (in **8**) crystallization molecule. Symmetry expansions reveal the *cis* geometry for compounds **2** and **3** and the *trans* configuration for the remaining ones. The nickel cations assume slightly distorted octahedral geometries (Table 2: angle variances [56] ranging from 23.44 to 50.26°²) constructed from the N_{pyridine}, and the N and the O-atoms from oxoquinoline. The NN lengths are in the expected double bond range. The Ni–N_{quinoline} distances vary from 2.049(3) to 2.087(3) Å (Table 2), being shorter than the Ni–N_{pyridine} which fluctuate between 2.112(3) and 2.1536(18) Å; complex **3** is the exception, with the latter dimension being larger than the former (values of 2.190(4) and 2.225(4) Å, against 2.153(4) and 2.168(4) Å, See Table 2) which is conceivably related to the geometry of the complex resulting in stereochemical effects from the 3-methylpyridine ligand. For the same reasons, the Ni–O distances in **3** are longer than those in the other compounds and the O–Ni–N_{quinoline} angles, as well as the nearby metal–metal distances, are markedly shorter (Table 2). The Ni–O dimensions measured in the present study are in the range of those already reported for quinolinate derivatives in Ni(II) octahedral environments [57], additionally with the Ni–N_{quinoline} length being longer than the Ni–O ones for the particular cases of *trans*-OO/*cis*-NN N_4O_2 nickel compounds [57b,57c] as found in **2** and **3**. The arylazo ligand in **1**, **4**, **5** and **7** is roughly planar as measured by the angle between the least-squares planes of the

quinoline and the phenyl moieties (angle P, see Table 2); while in the remaining compounds, however, it is markedly twisted. As expected, in view of their *cis* geometries in **2** and **3**, the angles between the least-squares planes of quinoline and pyridine (angle Q, see Table 2) are much shorter than in the other cases.

An interesting observation in the structures of **2** and **3** is the occurrence of intramolecular Ni...H_{pyridine} interactions. In these compounds, the pyridine ligand is clearly facing the metal, conceivably due to stereochemical effects from the 3-methylpyridine ligand (Figs. S3 and S4). Such twisting results in distances of 2.99 Å between the metal cation and the 6-H pyridine atom of both (in **2**) or just one (in **3**) 3-methylpyridine ligands, reasonably shorter than the lengths involving the 2-H pyridine atom which assume values between 3.02 and 3.12 Å in compounds of this work. According to the literature [58], these contacts are typical in metal-coordinated ligands interacting via lone pair dative bonds and sustain C–H...Ni longer than C...Ni, together with C–H...Ni angles shorter than 100° and may account for additional stabilization of the assemblies in **2** and **3** at least in the solid state.

The complex molecules in **1** are gathered through C–H...O

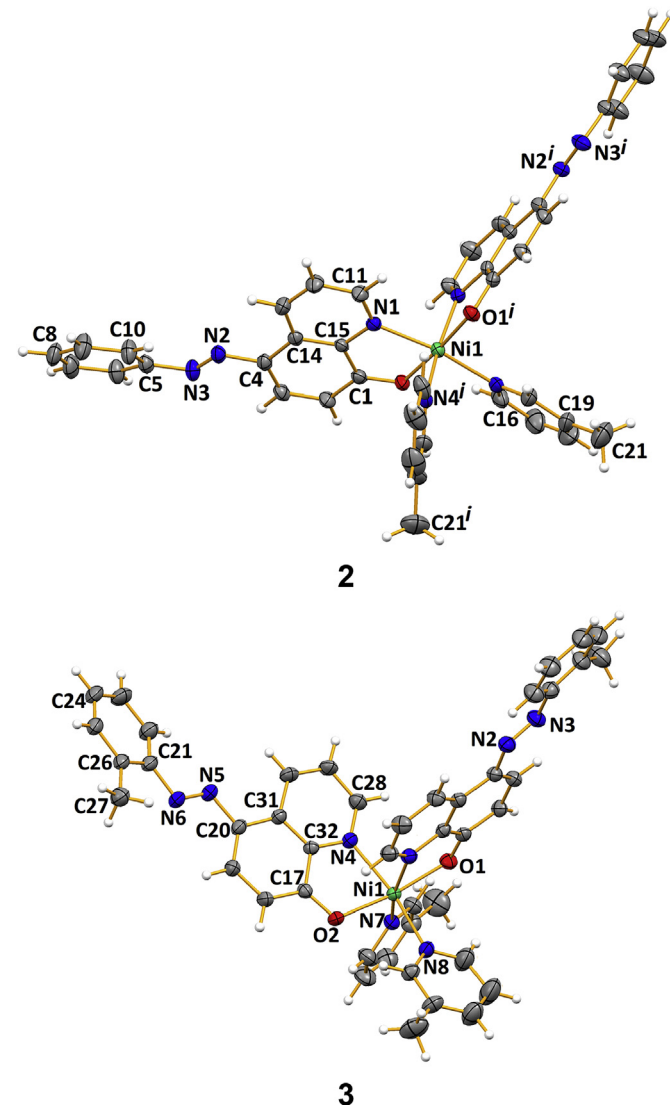


Fig. 2. Ellipsoid plot (drawn at 30% probability level) of the *cis* compounds **2** and **3**, with partial atom labelling schemes. Symmetry operation to generate equivalent atoms: 1.5-x,y,-z (**2**).

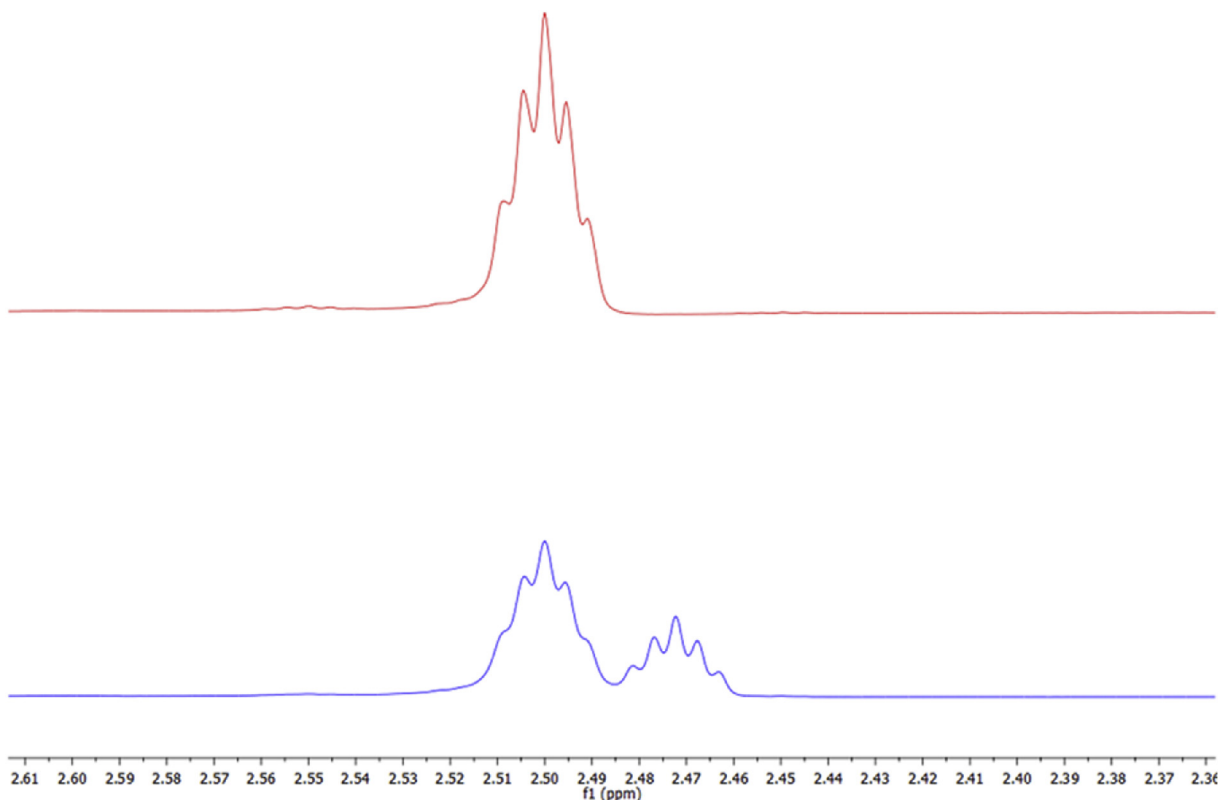


Fig. 3. ^1H NMR spectrum of DMSO- d_6 in the absence (top) and in the presence (bottom) of compound **8**.

contacts (Table 3) that give rise to infinite chains along the *c* axis ($\text{H}\cdots\text{O}$ and $\text{C}-\text{H}\cdots\text{O}$ of 2.70 Å, 171.3°) (Fig. S2). These chains create channels along the crystallographic *a* axis, which are filled with benzene solvent molecules. These trapped benzene molecules interact with four complex molecules by means of $\text{C}-\text{H}\cdots\pi$ contacts, donating to the pyridine ring and the phenyl moiety of quinoline from two adjacent molecules ($\text{H}\cdots\text{centroid}$ and $\text{C}-\text{H}\cdots\text{centroid}$ of 2.77 Å, 148° and 2.71 Å, 146°, in this order), and accepting from the pyridine moiety of quinoline from other two ($\text{H}\cdots\text{centroid}$ and $\text{C}-\text{H}\cdots\text{centroid}$ of 2.66 Å and 145°).

In complex **2**, the molecules are gathered by means of intermolecular contacts involving the pendent phenyl rings of azo group and the O-atoms giving rise to infinite 2D sheets (Fig. S3) owing to the *cis* geometry. Every molecule is additionally stabilized by means of intramolecular contacts between one of the pyridine H-atoms and the oxygen ($\text{H}\cdots\text{O}$ and $\text{C}-\text{H}\cdots\text{O}$ of 2.46 Å and 114°). In complex **3**, also with the *cis* geometry, the relevant interactions are of the intramolecular level (Fig. S4) with methyl pyridines donating to the O-atoms and β -quinoline to the N_{azo} .

The molecules of **7** are assembled in 2D sheets (Fig. S5) by means of the short contacts between a CH groups from pyridine and the O atoms from vicinal molecules. The halogen substituents (Br in **7**; Cl in **8**) also play a role in the stabilization of the structures: in **7** the Br establishes a π -interaction with the pyridine ring of a vicinal molecule ($\text{Br}\cdots\text{centroid}$ distance of 3.423 Å), while the Cl in **8** contacts with the methyl group of non-coordinated 3-methyl pyridine (Fig. S6).

3.3. Magnetic studies

Having now the availability of well-characterized series of octahedral Ni(II) compounds (**1–8**), it was thought of interest to

evaluate the solution behavior of these compounds. ^1H NMR spectra of **1–8** could not be obtained as anticipated in view of the paramagnetic character of the Ni(II). Recently [44], the effective magnetic moment (μ_{eff}) of Co(II) compounds of related system was determined using Evans method [48], which relates the difference in the chemical shift of an inert reference compound in the presence and in the absence of a paramagnetic species. The same methodology was adopted for determining μ_{eff} of the Ni(II) compounds **1–8** since the samples are highly soluble in DMSO whose sample preparation is straightforward and requires little material.

With DMSO- d_6 both as solvent and as internal standard its typical quintet was clearly shifted by the magnetic field of the Ni(II) paramagnetic compounds. An example of the obtained NMR spectra is shown in Fig. 3. The calculated magnetic moments, presented in Table 4 (refer to Table S2 for calculations), assume values between 3.02 and 3.40 BM which are in agreement with the expected values for Ni(II) cations in octahedral geometries with two unpaired electrons [59].

Table 4

Mass susceptibility, molar susceptibility and effective magnetic moment of compounds **1–8**.

Compound	χ_{mass} (cm^3/g)	χ_{mol} (cm^3/mol)	μ_{eff} (BM)
1	5.82×10^{-6}	4.61×10^{-3}	3.31
2	5.87×10^{-6}	4.36×10^{-3}	3.22
3	5.03×10^{-6}	3.87×10^{-3}	3.04
4	4.68×10^{-6}	3.83×10^{-3}	3.02
5	5.68×10^{-6}	4.84×10^{-3}	3.40
6	5.16×10^{-6}	4.54×10^{-3}	3.29
7	5.07×10^{-6}	4.82×10^{-3}	3.39
8	4.88×10^{-6}	4.86×10^{-3}	3.40

Table 5Antimicrobial activity of the pro-ligands (HL^{XAO}) and the nickel compounds (**1–8**) against representative bacterial and fungal strains.

Pro-ligand/Compound	Inhibition zones (in mm) observed for the tested bacterial and fungal species			
	<i>B. subtilis</i> MTCC 441	<i>S. aureus</i> MTCC 96	<i>K. pneumoniae</i> MTCC 109	<i>C. albicans</i> MTCC 183
HL ^H AQ	17	15	0	12
HL ^{2-MeAQ}	18	17	0	10
HL ^{4-MeAQ}	22	12	0	14
HL ^{4-OMeAQ}	12	0	0	10
HL ^{4-OEtAQ}	0	0	0	0
HL ^{4-BrAQ}	13	0	0	10
HL ^{4-CIAQ}	12	11	0	10
1	11	0	0	13
2	0	0	0	12
3	0	0	0	0
4	0	0	0	0
5	0	0	0	11
6	0	0	0	13
7	0	0	0	11
8	0	0	0	13
$\text{Ni(OAc)}_2 \cdot 4\text{H}_2\text{O}$	0	0	0	0
Solvent (10% DMSO)	0	0	0	0
Chloramphenicol (C) ³⁰	29	28	24	—
Fluconazole (FLC) ²⁵	—	—	—	26

3.4. Antibacterial activity results

The stability of compounds **1–8** in dimethyl sulfoxide (DMSO) solutions was monitored for two days (Fig. S7) and the observed unchanged pattern of the UV/Vis absorbance spectra indicated that the compounds are stable. The pro-ligands (except $\text{HL}^{\text{4-OEtAQ}}$) generally displayed less activity towards *B. subtilis* and *S. aureus* than bacterial control chloramphenicol (C)³⁰ while no activity was recorded for *K. pneumoniae*. However, the pro-ligands (except $\text{HL}^{\text{4-OEtAQ}}$) and compounds **1, 2, 5–8** demonstrated moderate activity against a fungal species *C. albicans* when compared with fluconazole (FLC)²⁵ (Table 5, Figs. S8 and S9). No systematic comparisons/correlations could be made when these results were compared with the analogous series of $[\text{Zn}(\text{L}^{\text{XAO}})_2(\text{yPy})_2]$ (yPy = pyridine or pyridine derivatives) complexes [44] since different bacterial stains were utilized. First-row transition metal compounds of 5-chloro-quinolin-8-olate were tested against bacteria, clinical isolates and probiotic bacteria and the results indicated that the zinc, cobalt and nickel compounds performed better activity than the positive control and the pro-ligand [60]. Thus, it may be inferred that the microbial activities of **1–8** can be related to several factors such as the type and number of donor atoms and their relative positions within the ligand [61].

4. Conclusion

Ni(II) complexes of the type $[\text{Ni}(\text{L}^{\text{XAO}})_2(\text{yPy})_2]$, where HL^{XAO} = substituted 5-[(*E*)-2-(aryl)-1-diazenyl]quinolin-8-olate; Py = pyridine or 3-methylpyridine, were synthesized and characterized. Single crystal X-rays diffraction studies revealed distorted octahedral geometries with *trans* configurations for **1, 4–8** and *cis* configurations for **2** and **3**. Intramolecular Ni...H_{pyridine} interactions are evident in the structures of **2** and **3** due to the geometry of the compounds. Magnetic moments studies in DMSO solutions are in agreement with Ni(II) cations in octahedral geometries with two unpaired electrons. The antimicrobial activity of the pro-ligands $\text{H}_2\text{L}^{\text{XASA}}$ and their Ni(II) compounds were studied in a comparative manner.

Conflicts of interest

The authors declare that they have no conflicts of interest with the contents of this article.

Acknowledgments

The financial support of the University Grants Commission, India (Grant No. 42–396/2013 (SR) 2013, TSBB), the Council of Scientific and Industrial Research, India (Grant No. 01 (2734)/13/EMR-II, 2013, TSBB) and the University Grants Commission, India, through SAP-CAS, Phase-I is gratefully acknowledged. KN thanks the University Grants Commission (UGC), India, for UGC-RGNF research fellowship. Authors (TSBB, KN) acknowledge DST-PURSE for the diffractometer facility. MFCGS and BGMR are grateful to the Foundation for Science and Technology (FCT), Portugal (UID/QUI/00100/2019).

Appendix A. Supplementary data

Supplementary data to this article can be found online at <https://doi.org/10.1016/j.molstruc.2019.127106>.

References

- [1] R.G.W. Hollingshead, Oxine and its Derivatives, vol. III, Butterworths Scientific Publications, London, 1956.
- [2] M. Albrecht, M. Fiege, O. Osetska, Coord. Chem. Rev. 252 (2008) 812–824.
- [3] D. Kalita, R. Herbst-Irme, D. Stalke, J.B. Baruah, Polyhedron 44 (2012) 52–58.
- [4] V. Prachayasittikul, S. Prachayasittikul, S. Ruchirawat, V. Prachayasittikul, Drug Des. Dev. Ther. 7 (2013) 1157–1178.
- [5] H.-L. Gao, S.-X. Jiang, Y.-M. Hu, F.-F. Li, Q.-Q. Zhang, X.-Y. Shi, J.-Z. Cui, Inorg. Chem. Commun. 44 (2014) 58–62.
- [6] I. Potočník, P. Vranec, V. Farkasová, D. Sabolová, M. Vataščinová, J. Kudláčová, I.D. Radojević, L.R. Čomić, B.S. Markovic, V. Volarevic, N. Arsenijevic, S.R. Trifunović, J. Inorg. Biochem. 154 (2016) 67–77.
- [7] H.-R. Zhang, T. Meng, Y.-C. Liu, Z.-F. Chen, Y.-N. Liu, H. Liang, Appl. Organomet. Chem. 30 (2016) 740–747.
- [8] V. Oliveri, G. Vecchio, Eur. J. Med. Chem. 120 (2016) 252–274.
- [9] C. Zhu, Y. Wang, Q. Mao, F. Li, Y. Li, C. Chen, Materials 10 (2017) 313, <https://doi.org/10.3390/ma10030313>.
- [10] V.A. Montes, G. Li, R. Pohl, J. Shinar, P. Anzenbacher Jr., Adv. Mater. 16 (2004) 2001–2003.
- [11] W. Chen, Q. Peng, Y. Li, Cryst. Growth Des. 8 (2008) 564–567.
- [12] H.C. Pan, F.P. Liang, C.J. Mao, J.J. Zhu, H.Y. Chen, J. Phys. Chem. 111 (2007) 5767–5772.

- [13] I.K. Yakushchenko, M.G. Kaplunov, S.S. Krasnikova, O.S. Roshchupkina, A.P. Pivovarov, Russ. J. Coord. Chem. 35 (2009) 312–316.
- [14] A.M. Baruah, R. Sarma, J.B. Baruah, Inorg. Chem. Commun. 11 (2008) 121–124.
- [15] M. Izquierdo, J. Casabó, C. Diaz, J. Ribas, Polyhedron 2 (1983) 529–536.
- [16] C. Engelter, G.E. Jackson, C.L. Knight, D.A. Thornton, J. Coord. Chem. 20 (1989) 289–306.
- [17] H. Kunkely, A. Vogler, Chem. Phys. Lett. 304 (1999) 187–190.
- [18] H. Kunkely, A. Vogler, J. Photochem. Photobiol. A Chem. 144 (2001) 69–72.
- [19] H. Kunkely, A. Vogler, Chem. Phys. Lett. 376 (2003) 226–229.
- [20] A. Strasser, A. Vogler, Inorg. Chim. Acta 357 (2004) 2345–2348.
- [21] H. Kunkely, A. Vogler, Inorg. Chim. Acta 362 (2009) 196–198.
- [22] L.S. Sapochak, A. Padmaperuma, N. Washton, F. Endrino, G.T. Schmett, J. Marshall, D. Fogarty, P.E. Burrows, S.R. Forrest, J. Am. Chem. Soc. 123 (2001) 6300–6307.
- [23] L. Li, B. Xu, Tetrahedron 64 (2008) 10986–10995.
- [24] L. Wang, X. Jiang, Z. Zhang, S. Xu, Displays 21 (2000) 47–49.
- [25] C.W. Tang, S.A. Van Slyke, Appl. Phys. Lett. 51 (1987) 913–915.
- [26] F.O. Suliman, I. Al-Nafai, S.N. Al-Busafi, Spectrochim. Acta 118 (2014) 66–72.
- [27] M. Albrecht, M. Fiege, O. Ossetska, Coord. Chem. Rev. 252 (2008) 812–824.
- [28] Y.-M. Hu, J. Qu, Y.-L. Yi, H.-L. Gao, J.-Z. Cui, J. Coord. Chem. 66 (2013) 18–27.
- [29] a) N. Donze, P. Pechy, M. Gratzel, M. Schaer, L. Zuppiroli, Chem. Phys. Lett. 315 (1999) 405–410;
b) Q.L. Huang, J.F. Li, T.J. Marks, J. Appl. Phys. 101 (2007), 093101;
- c) K. Sokolowski, I. Justyniak, W. Śliwiński, K. Sołtys, A. Tulewicz, A. Kornowicz, R. Moszyński, J. Lipkowski, J. Lewiński, Chem. Eur. J. 18 (2012) 5637–5645.
- [30] M.E. Mahmoud, S.S. Haggag, T.M. Abdel-Fattah, Polyhedron 28 (2009) 181–187.
- [31] L. Liu, L. Wang, D. Jia, J. Coord. Chem. 61 (2008) 1019–1026.
- [32] (a) T.S. Basu Baul, T.K. Chattopadhyay, B. Majee, Indian J. Chem., Sect. A 23 (1984) 470–474;
(b) I. Aiello, M. Ghedini, C. Zanchini, Inorg. Chim. Acta 255 (1997) 133–137;
(c) R. Sarkar, P. Mondal, K.K. Rajak, Dalton Trans. 43 (2014) 2859–2877;
(d) S.A. Abdel-Latif, H. Moustafa, Appl. Organomet. Chem. 31 (2017), e3876, <https://doi.org/10.1002/aoc.3876>.
- [33] E. El-Sawi, F.A. Moti, S. El-Messary, Bull. Soc. Chim. (Belg.) 94 (1985) 69–73.
- [34] T.S. Basu Baul, D. Dey, Synth. React. Inorg. Met. Org. Chem. 19 (1989) 101–112.
- [35] (a) K.D. Ghuge, P. Umapathy, M.P. Gupta, D.N. Sen, Inorg. Nucl. Chem. 43 (1981) 653–658;
(b) T.S. Basu Baul, T.K. Chattopadhyay, B. Majee, Polyhedron 2, 1983, pp. 635–640;
(c) B.K. Deb, A.K. Ghosh, Can. J. Chem. 65 (1987) 1241–1246;
(d) T.S. Basu Baul, A. Mizar, X. Song, G. Eng, R. Jirásko, M. Holčapek, R. Willem, M. Biesemans, I. Verbruggen, R. Butcher, J. Organomet. Chem. 691 (2006) 2605–2613;
(e) T.S. Basu Baul, A. Mizar, A. Lyčka, E. Rivarola, R. Jirásko, M. Holčapek, D. de Vos, U. Englert, J. Organomet. Chem. 691 (2006) 3416–3425;
(f) T.S. Basu Baul, A. Mizar, E. Rivarola, U. Englert, J. Organomet. Chem. 693 (2008) 1751–1758;
(g) T.S. Basu Baul, A. Mizar, A.K. Chandra, X. Song, G. Eng, R. Jirásko, Holčapek, D. de Vos, A. Linden, J. Inorg. Biochem. 102 (2008) 1719–1730;
(h) T.S. Basu Baul, A. Mizar, G. Ruisi, E.R.T. Tiekkink, Z. Anorg. Allg. Chem. 638 (2012) 664–668;
(i) T.S. Basu Baul, A. Mizar, G. Eng, R. Far, A. Linden, J. Coord. Chem. 66 (2013) 813–825.
- [36] T.S. Basu Baul, A. Mizar, A. Paul, G. Ruisi, R. Willem, M. Biesemans, A. Linden, J. Organomet. Chem. 694 (2009) 2142–2152.
- [37] A.Z. El-Sonbati, R.M. Issa, A.M. Abd El-Gawad, Spectrochim. Acta, Part A 68 (2007) 134–138.
- [38] M. Ghedini, M. La Deda, I. Aiello, A. Grisolia, J. Chem. Soc., Dalton Trans. (2002) 3406–3409.
- [39] M. La Deda, A. Grisolia, I. Aiello, A. Crispini, M. Ghedini, S. Belviso, M. Amati, F. Leij, J. Chem. Soc., Dalton Trans. (2004) 2424–2431.
- [40] F.-Y. Wu, X.-F. Tan, Y.-M. Wu, Y.-Q. Zhao, Spectrochim. Acta, Part A 65 (2006) 925–929.
- [41] (a) M. Hébrant, M. Rose-Hélène, J.-P. Joly, A. Walcarus, Colloids Surf., A 380 (2011) 261–269;
(b) M. Hébrant, M. Rose-Hélène, A. Walcarus, Colloids Surf., A 417 (2013) 65–72.
- [42] S.M. Seleim, T.A. Hamdalla, M.E. Mahmoud, Spectrochim. Acta, Part A 184 (2017) 134–140.
- [43] N.A. El-Wakil, H.F. Rizk, S.A. Ibrahim, Appl. Organomet. Chem. (2017) e3723, <https://doi.org/10.1002/aoc.3723>.
- [44] T.S. Basu Baul, K. Nongsiej, K. Biswas, S.R. Joshi, H. Höpfl, Inorg. Chim. Acta 482 (2018) 756–773.
- [45] T.S. Basu Baul, K. Nongsiej, B.G.M. Rocha, M.F.C. Guedes da Silva, J. Coord. Chem. 71 (2018) 2856–2874.
- [46] J.P. Thyssen, T. Menné, Chem. Res. Toxicol. 23 (2010) 309–318.
- [47] E. Denkhaus, K. Salnikow, Crit. Rev. Oncol. Hematol. 42 (2002) 35–56.
- [48] (a) D.F. Evans, J. Chem. Soc. (1959) 2003–2005;
(b) G.A. Bain, J.F. Berry, J. Chem. Educ. 85 (2008) 532–536;
(c) C. Piguet, J. Chem. Educ. 74 (1997) 815–816.
- [49] Agilent Technologies, XRD Products, Yarnton, Oxfordshire, England.
- [50] Agilent, CrysAlis PRO, Agilent Technologies Ltd, Yarnton, Oxfordshire, England, 2014.
- [51] A. Altomare, M.C. Burla, M. Camalli, G.L. Cascarano, C. Giacovazzo, A. Guagliardi, A.G.G. Moliterni, G. Polidori, R. Spagna, J. Appl. Crystallogr. 32 (1999) 115–119.
- [52] Crystal structure refinement with SHELXL, G.M. Sheldrick, Acta Crystallogr. C71 (2015) 3–8. <https://doi.org/10.1107/S2053229614024218>.
- [53] L.J. Farrugia, J. Appl. Crystallogr. 45 (2012) 849–854.
- [54] A.L. Spek, Acta Crystallogr. C 71 (2015) 9–18.
- [55] C. Perez, M. Paul, P. Bazerque, Acta Biol. Med. Exp. 15 (1990) 113–115.
- [56] K. Robinson, G.V. Gibbs, P.H. Ribbe, Science 172 (1971) 567–570.
- [57] (a) A.M. García-Deibe, J. Sanmartín-Matalobos, C. González-Bello, E. Lence, C. Portela-García, L. Martínez-Rodríguez, M. Fondo, Inorg. Chem. 51 (2012) 1278–1293;
(b) D. Mandal, C.S. Hong, H.C. Kim, H.-K. Fun, D. Ray, Polyhedron 27 (2008) 372–2378;
(c) A. Yuchi, M. Shiro, H. Murakami, H. Wada, G. Nakagawa, Bull. Chem. Soc. Jpn. 63 (1990) 677–686.
- [58] (a) D. Braga, F. Grepioni, E. Tedesco, K. Biradha, G.R. Desiraju, Organometallics 16 (1997) 1846–1856;
(b) M. Brookhart, M.L.H. Green, G. Parkin, Proc. Natl. Acad. Sci. 104 (2007) 6908–6914.
- [59] (a) F.A. Cotton, G. Wilkinson, Advanced Inorganic Chemistry, third ed., Wiley, New York, 1972, pp. 535–542;
(b) D.R. Eaton, K. Zaw, Can. J. Chem. 53 (1975) 633–643.
- [60] I. Potocnák, P. Vranec, V. Farkasová, D. Sabolová, M. Vataščinová, J. Kudláčová, I.D. Radović, L.R. Čomić, B.S. Marković, V. Volarević, N. Arsenijević, S.R. Trifunović, J. Inorg. Biochem. 154 (2016) 67–77.
- [61] S.H. Auda, I. Knutter, B. Bretschneider, M. Bransch, Y. Mrestani, C. Crobe, R.H.H. Neubert, Pharmaceuticals 2 (2009) 184–193.